NASA TECHNICAL NOTE

NASA TN D-5554

NASA TN D-5554

EXPLORATORY HEAT-TRANSFER MEASUREMENTS AT MACH 10 ON A 7.5° TOTAL-ANGLE CONE DOWNSTREAM OF A REGION OF AIR AND HELIUM TRANSPIRATION COOLING

by James C. Dunavant and Philip E. Everhart

Langley Research Center

Langley Station, Hampton, Va.

NATIONAL AERONAUTICS AND SPACE ADMINISTRATION • WASHINGTON, D. C. • DECEMBER 1969

EXPLORATORY HEAT-TRANSFER MEASUREMENTS AT MACH 10 ON A 7.5° TOTAL-ANGLE CONE DOWNSTREAM OF A REGION OF AIR AND HELIUM TRANSPIRATION COOLING

By James C. Dunavant and Philip E. Everhart
Langley Research Center

SUMMARY

The heat transfer to a 7.5° total-angle cone at a Mach number of 10 was measured to determine the far downstream effects of injecting air and helium into the cone boundary layer through a porous section near the apex. Transpiration rates varied from 0.0003 to 0.0084 times the flow rate through a stream tube equal to the maximum diameter of the model. The transpiration of both air and helium at these rates produced large increases in the pressure ratio over the transpiration region and expansion just downstream of the porous section to pressures well below those measured without transpiration. Over the rear half of the cone, the surface pressures returned to within approximately 10 percent of the pressure on the cone without transpiration. Large decreases in the heating were obtained just downstream of the transpiration region and resulted from injection of even small masses of coolant. Boundary-layer transition occurred earlier with air transpiration but was unaffected by helium transpiration. Where the flow was already turbulent, transpiration of air did not decrease the heating rates but helium caused a small decrease.

INTRODUCTION

Transpiration used to cool areas of intense local heating has not consistently reduced heating downstream of the transpiration area. While the addition of a cool gas to a boundary layer might be expected to reduce downstream temperatures and hence heat transfer, the thickening of the boundary layer from transpiration may cause earlier transition and high turbulent heating rates over areas that would experience lower laminar rates without injection. Exploratory tests were conducted to provide data on one arbitrarily selected configuration to measure downstream heating changes in a flow regime where the movement of transition could be observed. These tests further establish the variation in the magnitude of the downstream heating and transition with the specific heat of the injected gas.

A high-fineness-ratio cone with both air and helium injected into the boundary layer through a porous band near the apex was tested in the Mach 10 stream of the Langley

continuous-flow hypersonic tunnel. The model was a 7.5^{o} total-angle cone 69.38 inches (176 cm) in length with a porous band ahead of the 10 percent chord station. The area of the porous band was 11 percent of the base area, and the tests were conducted at mass injection rates from 0.0003 to 0.0084 times the flow rate through a stream tube equal to the base area. The tunnel stagnation pressure was varied from 25 to 95 atmospheres (2.4 to 9.6 MN/m^2) at an average temperature of 1028^{o} K resulting in free-stream Reynolds numbers (based on model length) from 2.7×10^6 to 10×10^6. Heating rates at 17 downstream stations on the model were determined from thermocouple time histories by using transient calorimeter techniques; heating rates are compared with those measured without injection.

SYMBOLS

A_b	area of cone base
c_p	specific heat of gas at constant pressure
c_w	specific heat of wall material
h	heat-transfer coefficient, $\frac{q}{T_{aw} - T_w}$
$\bar{h}$	average heat-transfer coefficient over cone surface
L	length of cone
$\dot{m}$	mass flow rate of coolant
N_{Pr}	Prandtl number
N_{St}	Stanton number, $\frac{h}{\rho_\infty u_\infty c_p}$
p	pressure
q	rate of heat flow per unit area
R	Reynolds number, $\frac{\rho_\infty u_\infty L}{\mu_\infty}$, based on model length
r	cone cross-sectional radius

s	distance along cone surface from apex
T	temperature
t	time
u	velocity
ϵ	emissivity
η	recovery factor
θ	cone half-angle
μ	viscosity
ρ	density
σ	Stefan-Boltzmann constant
τ	thickness of wall
ϕ	peripheral angle measured from top ray

Subscripts:

aw	adiabatic wall
e	effective
l	local
o	without transpiration coolant flow
t	stagnation

w wall

∞ free stream

Superscript:

' evaluated at reference temperature

APPARATUS AND TESTS

Facility

The tests were conducted in the Langley continuous-flow hypersonic tunnel which is capable of continuously maintaining a prescribed set of test conditions by recirculating the test air. To avoid liquefaction, the test air is heated by an electrical resistance tube heater before expansion through a contoured, three-dimensional, water-cooled nozzle to test conditions in a 31-inch-square (78.7-cm) test section. A sketch of the cone installed in the test section is shown in figure 1.

Models

Two models were tested. Both were sharp-tip, right circular cones with a total angle of 7.5°. The larger had a base diameter of 9 inches (22.86 cm); the smaller, a base diameter of 1.8 inches (4.6 cm). For both models, the diameter at the tip was 0.004 inch (0.012 cm). The larger cone, previously tested in the transition investigation of reference 1, was made from type 347 stainless steel and had a wall thickness of approximately 0.25 inch (0.635 cm). A porous section 3.5 inches long (8.89 cm) was formed of sintered type 316 stainless steel, with an approximate density of 0.152 lb/in^3 (4210 kg/m^3), and installed 3.8 inches (9.65 cm) from the apex. (See fig. 2.) The surface area of the porous section was 7.13 square inches (46 cm^2) with an average wall thickness of 0.125 inch (0.318 cm). For tests of this cone without transpiration, the porous section and cone tip were replaced with a nonporous conical piece.

An internal cooling system utilizing gaseous nitrogen at a temperature between 90° K and 170° K cooled the cone prior to the data-taking period. The nitrogen entered the cone through the sting mount and was distributed inside by a coolant tube shown in figure 2. Jets from this tube cooled the forward portion of the cone, and an internal conical shell caused the nitrogen to fan out and cool the rearward portion. After passing through the cone, the nitrogen was exhausted through the tunnel strut into the atmosphere.

The smaller cone, 13.75 inches (34.9 cm), which includes the porous section, was tested at stream flow and transpiration flow rates identical with those for the larger cone

to obtain pressures and schlieren photographs on the foward region. This cone had no internal cooling and was instrumented with seven pressure orifices. The smaller cone was centered in the test section (see fig. 1), and hence the tip was farther rearward in the tunnel than the tip of the large cone. The pressures measured without transpiration on this smaller cone were made without substituting a solid cone section for the porous section as was done on the larger cone.

Air and helium were injected through the porous section. The transpiration coolants passed through separate supply lines to a three-way solenoid valve and then used the same 0.25-inch (0.635-cm) line to reach the plenum of the porous section. This line extended through the sting mount inside the gaseous nitrogen coolant tube. At the time of the heat-transfer measurements, the temperature in the plenum of the porous section was between 240° K and 310° K for helium and between 210° K and 280° K for air. Air flow rates were determined by using a turbine-type flowmeter in conjunction with the measured pressure and temperature of the coolant. Helium flow rates were metered through a calibrated sharp-edge orifice. The maximum inaccuracy of flow measurements was estimated to be ±7 percent for air and ±12 percent for helium.

Instrumentation

The large cone was instrumented with 116 thermocouples and 21 pressure orifices, the locations of which are given in table I. Number 30 gage wire chromel-alumel thermocouples were installed in five rows along the model surface beginning approximately 5.7 inches (14.5 cm) downstream of the end of the porous section. Details of the thermocouple installation are shown in figure 2. Two thermocouples were installed in the transpiration section to measure the porous wall temperature and the temperature of the coolant in the plenum. Thermocouple outputs were automatically recorded on magnetic tape by an analog-to-digital converter. The reference temperature of each thermocouple was maintained at 325° K.

The 0.040-inch-diameter (0.102-cm) pressure orifices on the large cone were installed primarily along the bottom ray of the cone ($\phi = 180^{\circ}$), starting approximately 7.7 inches (19.6 cm) aft of the porous section. Several pressure orifices were installed along other rays to provide a check on the symmetry of the flow. The locations for the seven pressure orifices on the small cone are given in table II. One orifice was located ahead of the transpiration section, three in the transpiration section, and three behind the section. The large cone is uninstrumented in this region. Orifices were connected through two 12-port scanner valves to two capacitance-type, multirange transducers whose outputs were recorded by an analog-to-digital data system.

Tests and Procedure

Tests were conducted at tunnel stagnation pressures of approximately 350 psia (2.4 MN/m^2), 700 psia (4.8 MN/m^2), and 1400 psia (9.6 MN/m^2) with corresponding nominal free-stream Mach numbers of 10.1, 10.3, and 10.4, respectively. The average tunnel stagnation temperature was 1028° K. The range of free-stream Reynolds number was from about 0.47×10^6 to 1.75×10^6 per foot (1.54×10^6 to 5.74×10^6 per meter).

Prior to recording data, the cone was cooled in the tunnel with gaseous nitrogen to a temperature on the order of 270° K. When the desired tunnel condition was reached, the transpiration mass flow rate was set, the internal cooling was stopped, and after several minutes delay the temperature of the model wall was recorded at 1-second intervals. Data for zero injection were obtained in separate tests by using a solid cone section in place of the porous section.

The convective heat-transfer coefficient h, defined in terms of the heat input to the cone, was calculated from the temperature-time histories at the thermocouple locations and corrected for radiation to and from the tunnel walls which were at approximately 300° K by using the following equation:

$$q = h\left(T_{aw} - T_w\right) = \rho_w c_w \tau_e \frac{dT_w}{dt} + \left(\epsilon\sigma T_w^4\right)_{model} - \left(\epsilon\sigma T_w^4\right)_{tunnel}$$

The temperature-time derivative dT_w/dt was determined by first fitting a quadratic least-square curve to the measured data, differentiating this curve, and then evaluating the result at the desired time. The values of the density ρ_w and specific heat c_w of the wall material were taken to be 0.290 lb/in^3 (8030 kg/m^3) and 0.120 Btu/lb-$^{\circ}$F (502.1 J/kg-$^{\circ}$K), respectively. Values of the effective wall thickness, calculated from the equation $\tau_e = \tau - \frac{\tau^2}{2r}$ by using values measured during the construction of the cone, varied from 0.223 to 0.256 inch (0.566 to 0.650 cm). The measured emissivity ϵ of the cone was 0.23 for the range of wall temperatures of interest.

The adiabatic-wall temperature was obtained from the equation

$$T_{aw} = \eta\left(T_t - T_l\right) + T_l$$

For simplicity, a recovery factor η of 0.84 was used for all data reduction. Although heating rates were calculated from the temperatures measured by all the surface thermocouples, only a limited number of the main ray temperatures and heating rates which are representative of the results are presented herein.

Estimates of heat conduction along the surface of the cone were made to determine the effect on the measured heating. One-dimensional heat conducted longitudinally was

calculated by using a three-point finite-difference method to determine the second derivative of the wall temperature with distance. The results of these calculations made at selected stations having maximum values of the second derivative showed that conduction contributes less than 10 percent to the measured heating rates; all results are presented without corrections for conduction.

RESULTS AND DISCUSSION

Flow Field

Pressures measured on the cone surface at an angle of attack of 0° are shown for the various flow rates and the three Reynolds numbers in figure 3 for air and helium injection. The pressures at the first seven stations were obtained on the short cone and the remainder on the large cone. As noted previously, the results shown for $\frac{\dot{m}}{\rho_{\infty}u_{\infty}A_b} = 0$ on the large cone were obtained with the solid tip section in place of the porous section; on the shorter cone, the porous section was in place. No appreciable effect of these model variations or model location in the test section can be observed in the results for $\frac{\dot{m}}{\rho_{\infty}u_{\infty}A_b} = 0$; the largest apparent change in pressure from the small cone to the large cone is an increase of about 12 percent and occurs at the highest Reynolds number. The pressures ahead of the porous section are greater than the inviscid pressures given by Kopal in reference 2, and this difference can be only partly accounted for by calculated viscous-induced pressure.

Over the porous section, the pressure reached 2 to 5 times that without transpiration; the higher values occurred when helium was used. The cone shock shown in a typical schlieren photograph in figure 4(a) is curved over the porous section and displaced outward at an angle about twice that expected for a cone without transpiration. Interpretations of the transpiration flow fields are shown in figures 4(b) and 4(c). The pressures measured at the one orifice on the short solid cone forward of the porous section are usually unaffected by transpiration. However, at several of the higher injection rates this pressure increases abruptly as a result of the flow separation illustrated in figure 4(c). The high pressure over the porous surface produces a forward flow of some of the low-velocity injected gas, that is, a reverse flow layer adjacent to the surface which is similar to a laminar separation flow. The extent of this separation can be determined only for the few conditions in which the separation moves forward, covers the most forward orifice, and produces the abrupt pressure increase. As is typical of laminar separation, the region is larger at high Reynolds numbers.

The formation of a boundary or mixing region between the stream and the injected gas starts approximately at the forward edge of the porous section and is visible for a

considerable distance downstream. The pressure decreases rapidly and thus accelerates the transpiring gas to supersonic speeds even though it was injected with no streamwise velocity. The layer of injected gas is thickest at the trailing edge of the porous section and thins downstream because of the conical flow effect and acceleration in the favorable pressure gradient which exists for the next 8 inches (20 cm) along the cone surface. The curved boundary between the transpiration flow and the stream allows an expansion of the inviscid flow just downstream of the porous region to pressures lower than those without transpiration. The boundary layer negotiates an adverse pressure gradient on the cone to reach pressures on the rear half of the cone which are within approximately 10 percent of the pressure at $\frac{\dot{m}}{\rho_\infty u_\infty A_b} = 0$. A further indication of the extent of the disturbance to the flow in the region of transpiration was the movement of the conical shock whose angle, measured from the cone surface, approximately doubled at the highest transpiration rate. Even though transpiration does cause substantial changes in the inviscid flow immediately downstream of the transpiration region, the effects on the pressure over the rear half of the cone are small (less than 10 percent).

Heat Transfer

Wall temperatures.- Wall-temperature distributions at the time the heating rate was measured are shown in figure 5(a) for air transpiration and in figure 5(b) for helium transpiration. The nonuniform wall-temperature distribution is a result of the distribution of temperature which exists at the end of the cooling cycle. Although the temperature level increases during the test period, little change takes place in the shape of the distributions.

Air transpiration.- Longitudinal distributions of the measured Stanton number at the various transpiration rates are shown in figure 6 for air transpiration. Figures 6(a), 6(b), and 6(c) represent model length Reynolds numbers of 2.84×10^6, 5.21×10^6, and 10.22×10^6, respectively. The Stanton number measured on the cone with a solid tip to represent the condition of zero transpiration rate is shown for comparison.

Although the heating rate immediately downstream of the porous region was sharply reduced by the injection of either air or helium, the cooling effectiveness varied widely with increased distance from the porous area. Theories which are available for predicting a variation in cooling effectiveness with distance from the point of injection are restricted to low flow rates and cannot account for changes in character of the flow. The high flow rates and Reynolds numbers of the present tests resulted in major changes in the character of the external flow over the transpiration region and just downstream.

Irregularities in the heating near the midpoint of the cone are largely unexplained. In many cases, they appear to be related to the temperature discontinuities in this area. (See fig. 5.)

The solid-tip cone model was previously used to study transition in reference 1. In that investigation the beginning of transition was taken as the location where the slope of the faired data distribution first deviated significantly from the slope of the laminar theory and continued this deviation downstream. Thus from reference 1, transition without transpiration starts at $s = 34$ inches (86 cm) at $R = 5.21 \times 10^6$ (fig. 6(b)) and at $s = 22$ inches (56 cm) for $R = 10.22 \times 10^6$ (fig. 6(c)). At the lowest Reynolds number of 2.84×10^6, a transition Reynolds number can be deduced from the variation with unit Reynolds number which would place the start of transition at $s = 54$ inches (137 cm). Again from reference 1, transition is observed to occur slowly over a flow length of 1 to $1\frac{1}{2}$ times the length of the laminar boundary layer. Theoretical predictions of laminar and turbulent heating[1] without transpiration are presented with the test results for reference.

The injection of air into the boundary layer was shown in all of these tests to result in heating rates over much of the aft portion of the model higher than those obtained without air injection. The injected air appears to have produced transition; the point of transition, however, is not clearly defined. In figure 6, transition with transpiration occurs far ahead of that without transpiration and is little affected by transpiration flow rate over the range of these tests. The location, however, moves forward with increasing Reynolds number.

At the highest Reynolds number, where a fully turbulent boundary layer exists without transpiration, the heating rates near the trailing edge are equal to those without transpiration. Thus it appears that when turbulent flow already exists, transpiration of air has negligible effect on the heating rate.

Helium transpiration.- The heat transfer with helium transpiration is shown in figure 7 and differs markedly from that with air transpiration. At the lowest Reynolds number (fig. 7(a)), the heating at all transpiration rates is less than the laminar heating without transpiration. The considerable reduction in heating at all transpiration rates persists for the full length of the cone at the lowest Reynolds number (fig. 7(a)). The boundary layer with transpiration is believed laminar for the entire length of the cone at $R = 2.84 \times 10^6$ (fig. 7(a)). For each of the four transpiration rates shown in figure 7(a), the heating at the trailing edge is about one-half that without transpiration in spite of a variation in coolant injection rates by a factor of 4.

---

[1]The theoretical laminar heating rates used herein are determined from the Monaghan reference temperature relation (ref. 3), the Blasius skin-friction relationship, and the Colburn-Reynolds analogy. The turbulent rates shown in figures 6 and 7 are obtained from the Monaghan reference temperature relationship of reference 4 and the relationship $N'_{St}(R')^{1/5} = 0.0592/2\left(N'_{Pr}\right)^{2/3}$. The flow was considered to be turbulent from the apex, and a factor of 1.15 was used to account for the difference between flat-plate and cone heating. Thus, both predictions are identical with that used in reference 1 to find transition initially on the solid-tip cone.

At the two higher Reynolds numbers (figs. 7(b) and 7(c)), where transitional and turbulent heating rates are present without transpiration, the heating for all helium transpiration rates exceeds the theoretical laminar heating near the trailing edge and is slightly less than the heating without transpiration. Thus, as for air, helium transpiration is ineffective as a coolant downstream of transition; however, with helium transpiration, the location of transition, as defined by the heating rates, is not moved forward. Theoretical results in reference 5 and experimental results in reference 6 have shown that injection of helium has a stronger effect than injection of heavier gases on the movement of transition over the region of transpiration cooling. In reference 7, downstream of the porous region, transition was farther forward with nitrogen injection than with helium injection. In that experiment, the coolant was injected through the hemispherical portion of a nose cone.

Downstream heating change.- The change in heat transfer effected by the addition of air and helium to the boundary layer is shown in figure 8 where transpiration rates are plotted as functions of longitudinal position on the cone for each of the three Reynolds numbers. The results are shown as contours of constant values of the ratio of the heat-transfer coefficient with transpiration to that without h/h_0.

Air transpiration (fig. 8(a)) causes large decreases in the heating over the forward part of the cone; the region of reduced heating is smaller at the higher Reynolds numbers. Farther rearward, the heating with transpiration exceeds that without transpiration; that is h/h_0 is greater than 1.0, and although the contour of $h/h_0 = 1.0$ moves forward with increasing Reynolds number, its location is unaffected by the various transpiration rates of these tests. Values of h/h_0 as high as 2 are present in the air results (fig. 8(a)) over the regions where transition with transpiration is ahead of that without. Aft of the transition region air injection has little effect and h/h_0 decreased toward 1.0.

The helium results shown in figure 8(b) exhibit much longer regions of reduced heating than were observed with air. At $R = 2.84 \times 10^6$, this condition extends over the entire cone. Only at the highest Reynolds number are values of $h/h_0 > 1.0$ obtained. If the anomalous behavior of wall temperature at approximately the midpoint of the cones had not occurred, all values of h/h_0 for helium would have been less than 1.0.

Net cooling effect of transpiration.- Air transpiration has shown a strong cooling effect immediately behind the transpiration section followed by transition in the boundary layer with high heating rates. To illustrate the net effect of transpiration on the total heat load to the cone, the heating rates over the cone surface area were graphically integrated and are shown in figure 9 as the ratio of average heat-transfer coefficient with transpiration to average heat-transfer coefficient without transpiration. The greater effectiveness of helium as a coolant is shown by the fact that the values of $\bar{h}/\bar{h}_0$ are all less than 1 and thus indicate a decrease in heating. With air as a coolant, $\bar{h}/\bar{h}_0$ is

always greater than 1 not just because air is less effective as a coolant, but also because it promotes earlier transition. If the heating for lengths less than the full length of the cone were considered, the heating ratio $\bar{h}/\bar{h}_o$ would be much different. For example, if only a short region immediately downstream of the transpiration region were considered, both air and helium injection would show large reductions in the cone heating, with helium showing the greater reduction. Thus, the results shown in figure 9 cannot be generalized but are relevant only for the specific configuration and the test conditions of this investigation and indicate that transpiration may produce increases in the heat load if the transpiration promotes early transition.

SUMMARY OF RESULTS

An investigation of the heat transfer to a 7.5^o total-angle cone at a Mach number of 10 has been made to determine the far downstream effects of injecting air and helium into the cone boundary layer through a porous section near the apex. The tests were made at free-stream Reynolds numbers based on model length of 2.84×10^6, 5.21×10^6, and 10.22×10^6. Transpiration rates varied from 0.0003 to 0.0084 times the flow rate through a stream tube equal to the maximum diameter of the model.

1. The transpiration of both air and helium at the transpiration rates of these tests produced large increases in the pressure over the transpiration region. The local disturbance to the flow resulted in an overexpansion region just downstream of the transpiration section. Over the rear half of the cone the surface pressures at all transpiration flow rates had returned to within approximately 10 percent of the cone pressure without transpiration.

2. Large decreases in the heating were obtained just downstream of the transpiration region. The region of heating reduction was approximately independent of transpiration rate but decreased at the higher Reynolds numbers. The region of decreased heating was larger for helium and extended to the trailing edge at the lowest Reynolds number.

3. Boundary-layer transition downstream of the transpiration region occurred earlier with air transpiration but was apparently unaffected by helium transpiration. This transition movement is unlike the change in location when transition occurs over the region of transpiration; here injection of a light gas produces the earlier transition.

4. Where the flow was turbulent, transpiration of air did not decrease the heating rates but helium caused a small decrease.

5. Although transpiration always appeared effective in reducing the heating rate immediately behind the transpiration region, the total heating for the cone increased with air transpiration because transition moved forward. Helium transpiration reduced the total heating to the cone.

Langley Research Center,
National Aeronautics and Space Administration,
Langley Station, Hampton, Va., April 10, 1969.

REFERENCES

1. Everhart, Philip E.; and Hamilton, H. Harris: Experimental Investigation of Boundary-Layer Transition on a Cooled 7.5° Total-Angle Cone at Mach 10. NASA TN D-4188, 1967.

2. Staff of Comput. Section, Center of Anal. (Under dir. of Zdeněk Kopal): Tables of Supersonic Flow Around Cones. Tech. Rep. No. 1 (NOrd Contract No. 9169), Massachusetts Inst. of Technol., 1947.

3. Monaghan, R. J.: An Approximate Solution of the Compressible Laminar Boundary Layer on a Flat Plate. R. & M. No. 2760, Brit. A.R.C., 1953.

4. Monaghan, R. J.: On the Behavior of Boundary Layers at Supersonic Speeds. Fifth International Aeronautical Conference, Rita J. Turino and Caroline Taylor, eds., Inst. Aeron. Sci., Inc., June 1955, pp. 277-315.

5. Gross, J. F.; Hartnett, J. P.; Masson, D. J.; and Gazley, Carl, Jr.: A Review of Binary Laminar Boundary Layer Characteristics. Int. J. Heat Mass Transfer, vol. 3, no. 3, Oct. 1961, pp. 198-221.

6. Pappas, Constantine C.; and Okuno, Arthur F.: Measurements of Skin Friction of the Compressible Turbulent Boundary Layer on a Cone with Foreign Gas Injection. J. Aero/Space Sci., vol. 27, no. 5, May 1960, pp. 321-333.

7. Cresci, Robert J.; and Libby, Paul A.: The Downstream Influence of Mass Transfer at the Nose of a Slender Cone. J. Aerosp. Sci., vol. 29, no. 7, July 1962, pp. 815-826.

TABLE I.- ORIFICE AND THERMOCOUPLE LOCATIONS

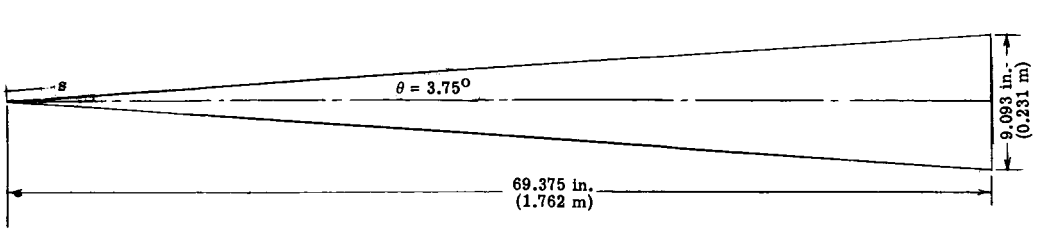

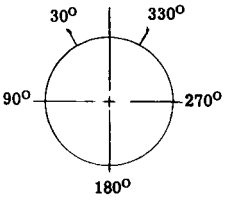

Thermocouple	s		φ, deg	Thermocouple	s		φ, deg	Orifice	s		φ, deg
	in.	m			in.	m			in.	m	
1	13.00	0.330	0	59	51.00	1.295	30	1	15.00	0.381	180
2	13.00	.330	90	60	52.00	1.321	330	2	20.00	.508	0
3	16.00	.406	0	61	52.00	1.321	0	3	20.00	.508	90
4	19.00	.483	0	62	52.00	1.321	30	4	20.00	.508	180
5	19.00	.483	90	63	53.00	1.346	330	5	25.00	.635	180
6	22.00	.559	0	64	53.00	1.346	0	6	30.00	.762	0
7	25.00	.635	0	65	53.00	1.346	30	7	30.00	.762	90
8	28.00	.711	0	66	53.75	1.365	180	8	30.00	.762	180
9	28.00	.711	90	67	54.00	1.372	330	9	35.00	.889	180
10	31.00	.787	0	68	54.00	1.372	0	10	40.00	1.016	180
11	32.50	.826	0	69	54.00	1.372	30	11	42.50	1.080	180
12	34.00	.864	0	70	55.00	1.397	330	12	45.00	1.143	180
13	35.50	.902	0	71	55.00	1.397	0	13	47.50	1.207	180
14	37.00	.940	330	72	55.00	1.397	30	14	50.00	1.270	180
15	37.00	.940	0	73	56.00	1.422	330	15	52.50	1.334	180
16	37.00	.940	30	74	56.00	1.422	0	16	55.00	1.397	180
17	37.00	.940	90	75	56.00	1.422	30	17	57.50	1.461	180
18	38.50	.978	330	76	56.75	1.441	180	18	60.00	1.524	180
19	38.50	.978	0	77	57.00	1.448	330	19	62.50	1.588	180
20	38.50	.978	30	78	57.00	1.448	0	20	65.00	1.651	180
21	40.00	1.016	330	79	57.00	1.448	30	21	67.50	1.715	180
22	40.00	1.016	0	80	58.00	1.473	330				
23	40.00	1.016	30	81	58.00	1.473	0				
24	40.00	1.016	90	82	58.00	1.473	30				
25	41.00	1.041	330	83	58.75	1.492	180				
26	41.00	1.041	0	84	59.00	1.499	330				
27	41.00	1.041	30	85	59.00	1.499	0				
28	42.00	1.067	330	86	59.00	1.499	30				
29	42.00	1.067	0	87	60.00	1.524	330				
30	42.00	1.067	30	88	60.00	1.524	0				
31	43.00	1.092	330	89	60.00	1.524	30				
32	43.00	1.092	0	90	60.00	1.524	90				
33	43.00	1.092	30	91	61.00	1.549	330				
34	44.00	1.118	330	92	61.00	1.549	0				
35	44.00	1.118	0	93	61.00	1.549	30				
36	44.00	1.118	30	94	62.00	1.575	330				
37	45.00	1.143	330	95	62.00	1.575	0				
38	45.00	1.143	0	96	62.00	1.575	30				
39	45.00	1.143	30	97	63.00	1.600	330				
40	46.00	1.168	330	98	63.00	1.600	0				
41	46.00	1.168	0	99	63.00	1.600	30				
42	46.00	1.168	30	100	63.75	1.619	180				
43	47.00	1.194	330	101	64.00	1.626	330				
44	47.00	1.194	0	102	64.00	1.626	0				
45	47.00	1.194	30	103	64.00	1.626	30				
46	48.00	1.219	330	104	65.00	1.651	330				
47	48.00	1.219	0	105	65.00	1.651	0				
48	48.00	1.219	30	106	65.00	1.651	30				
49	48.75	1.238	180	107	65.00	1.651	90				
50	49.00	1.245	330	108	66.00	1.676	330				
51	49.00	1.245	0	109	66.00	1.676	0				
52	49.00	1.245	30	110	66.00	1.676	30				
53	50.00	1.270	330	111	67.00	1.702	330				
54	50.00	1.270	0	112	67.00	1.702	0				
55	50.00	1.270	30	113	67.00	1.702	30				
56	50.00	1.270	90	114	68.00	1.727	330				
57	51.00	1.295	330	115	68.00	1.727	0				
58	51.00	1.295	0	116	68.00	1.727	30				

TABLE II.- ORIFICE LOCATIONS ON SHORT CONE

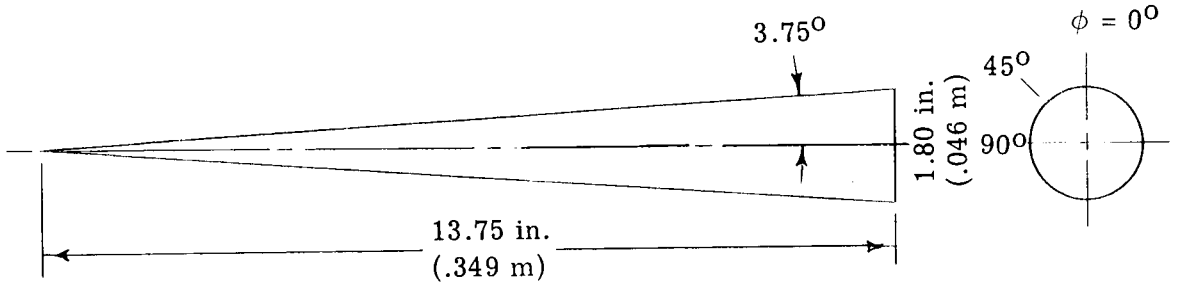

Orifice	s		φ, deg
	in.	m	
1	1.914	0.049	0
2	4.710	.120	0
3	5.592	.142	45
4	6.474	.164	90
5	8.949	.227	0
6	10.563	.268	45
7	12.176	.309	90

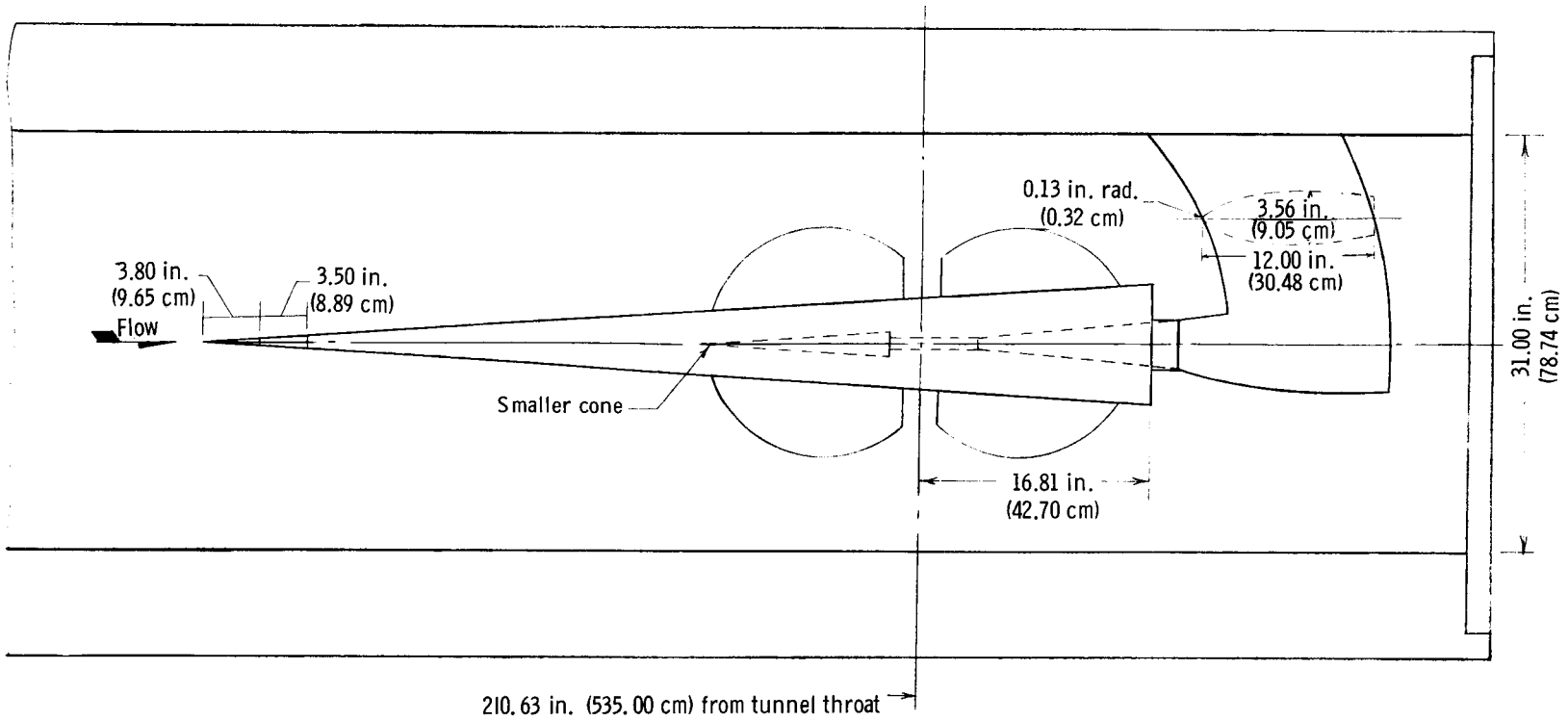

Figure 1.- Sketch of typical installation of cone model in tunnel.

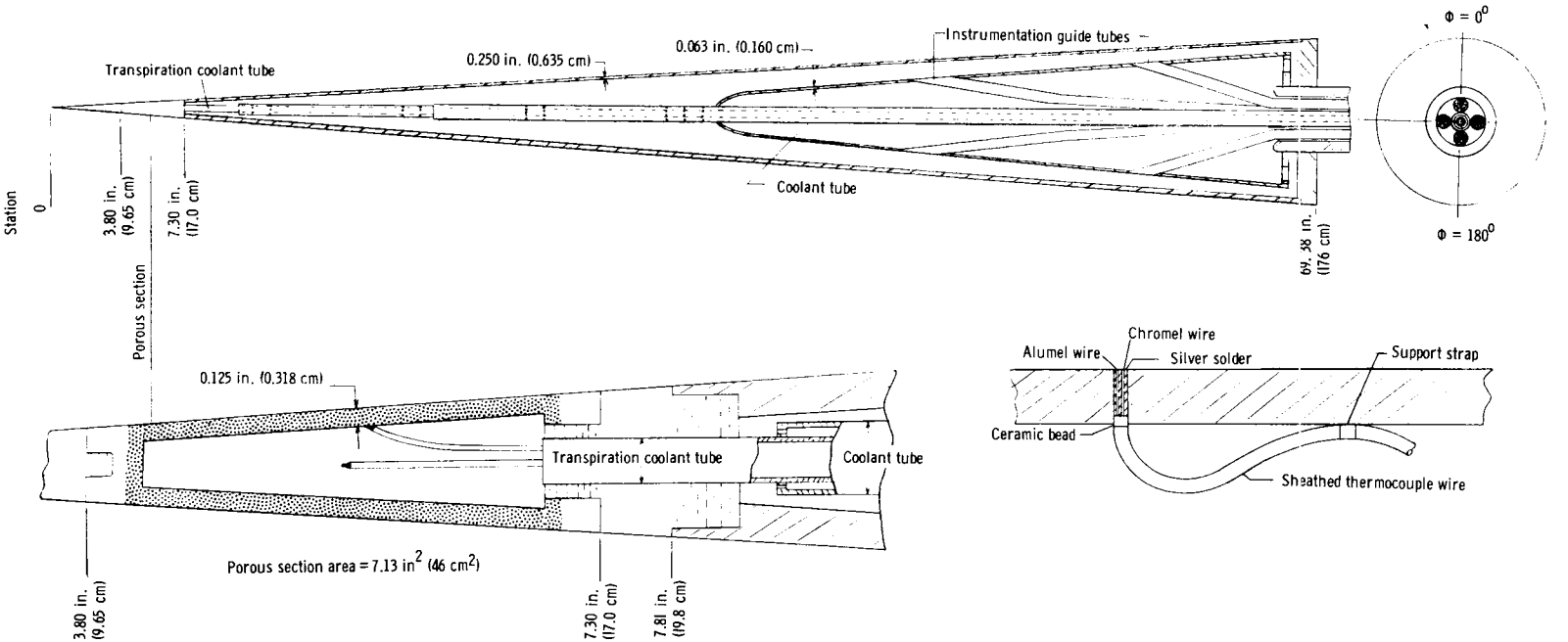

Figure 2.- Sketch of cone showing porous section, coolant tubes, and thermocouple installation.

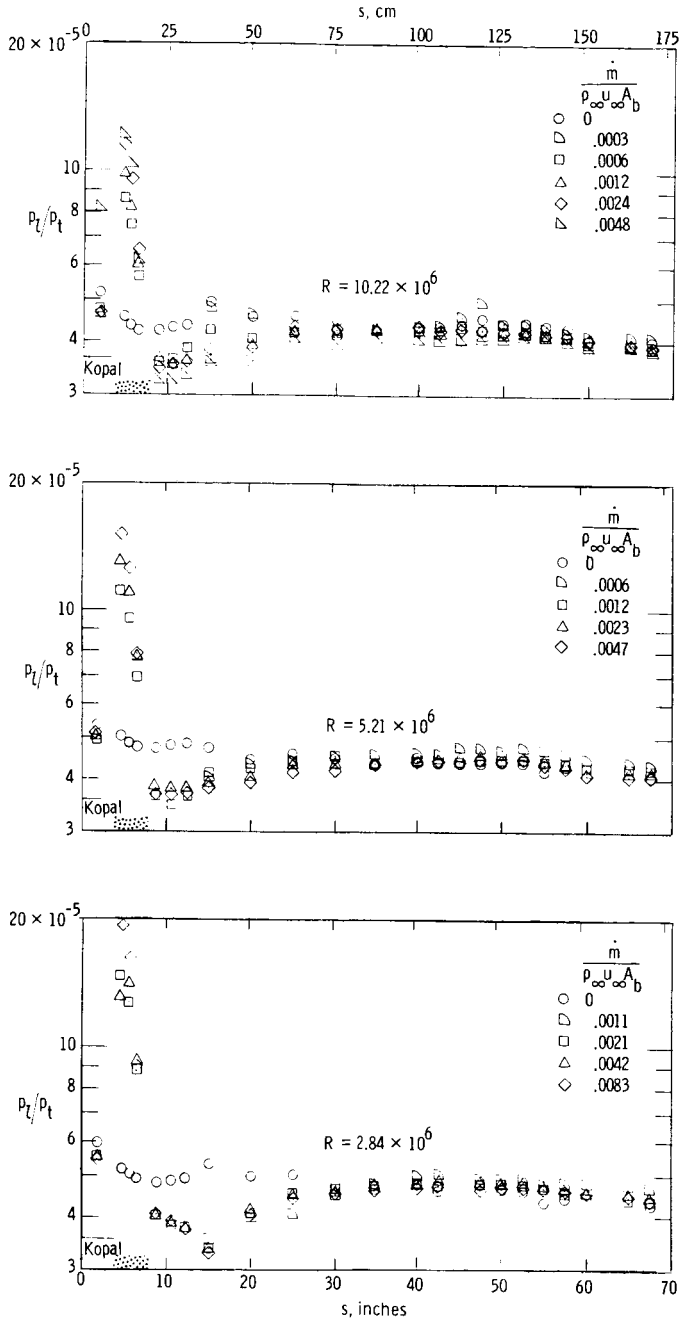

(a) Air.

Figure 3.- Pressure distribution along the cone surface.

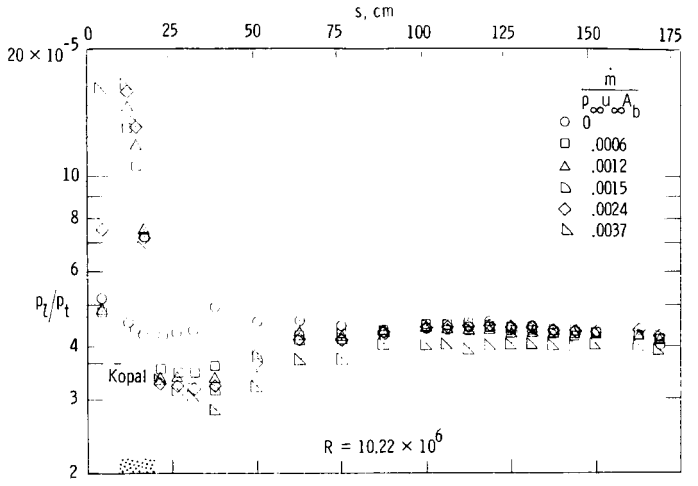

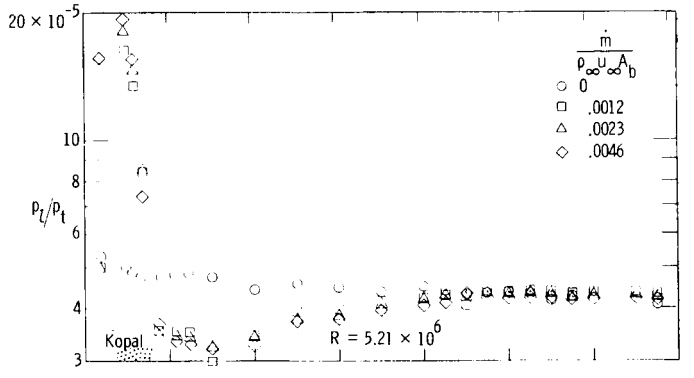

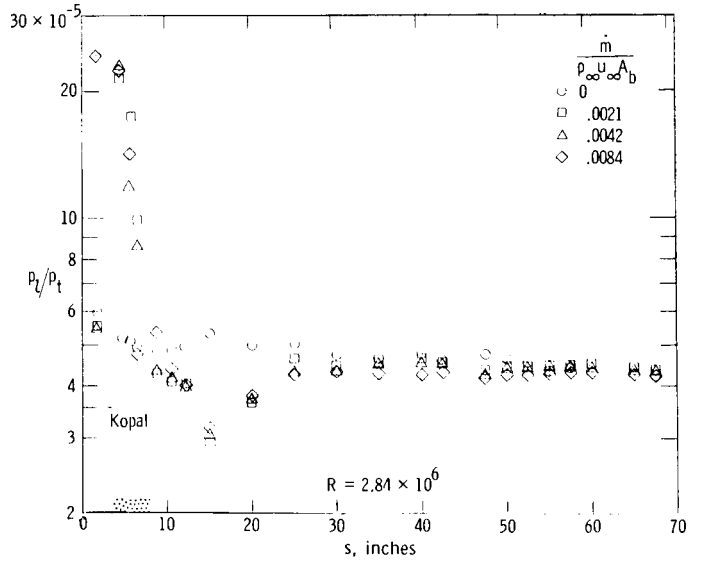

(b) Helium.

Figure 3.- Concluded.

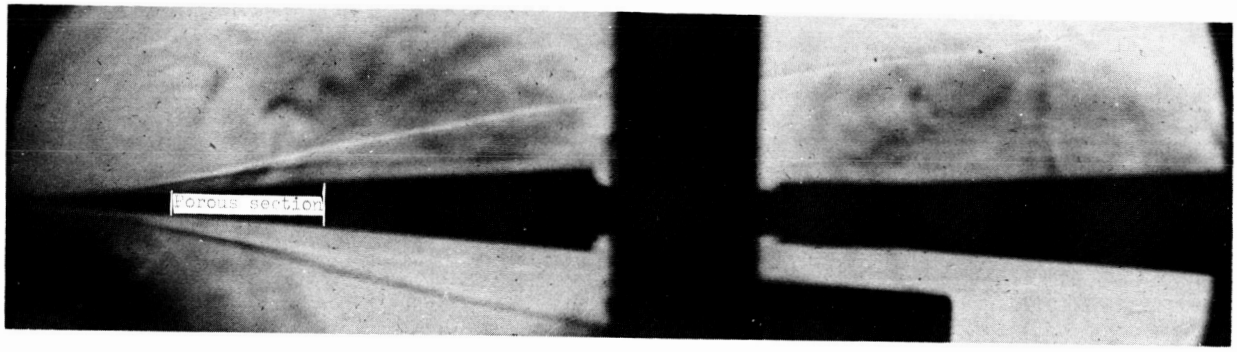

(a) Schlieren photograph. $R = 10.22 \times 10^6$; $\frac{\dot{m}}{\rho_\infty u_\infty A_b} = 0.0012$ (helium).

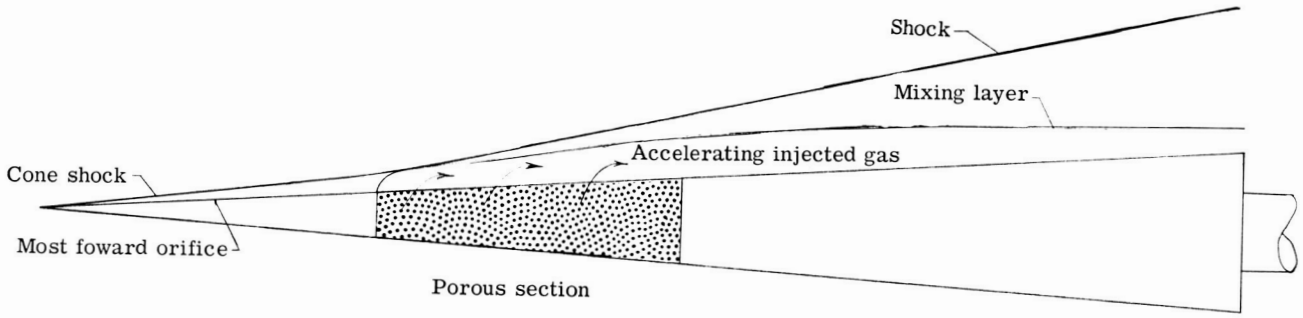

(b) Transpiration flow field.

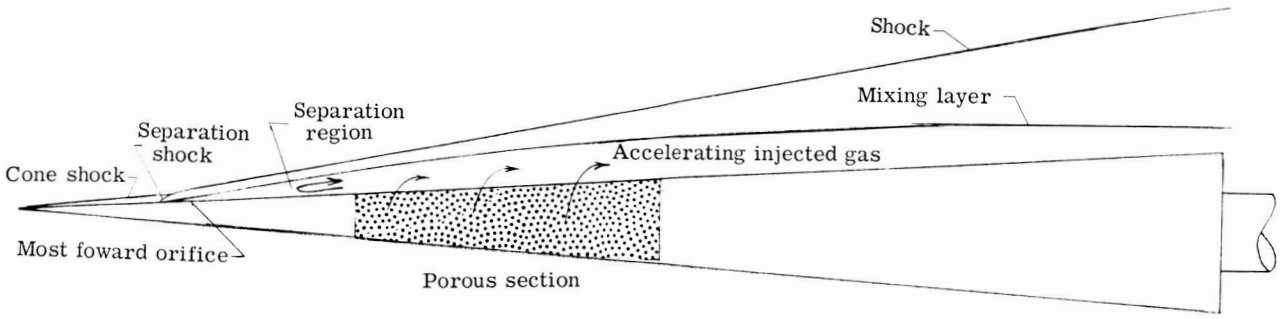

(c) Transpiration-induced separation.

Figure 4.- Flow fields on short cone.

L-69-1352

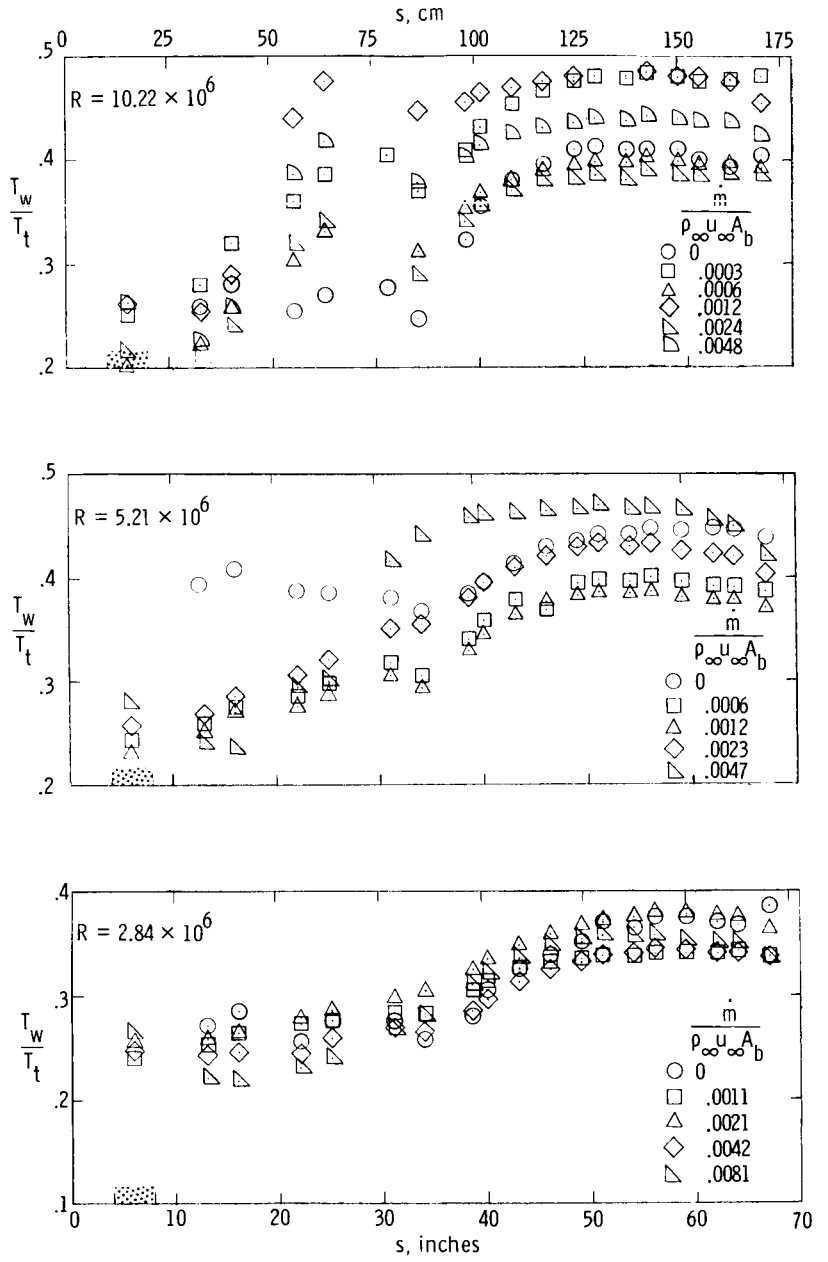

(a) Air.

Figure 5.- Wall-temperature distribution.

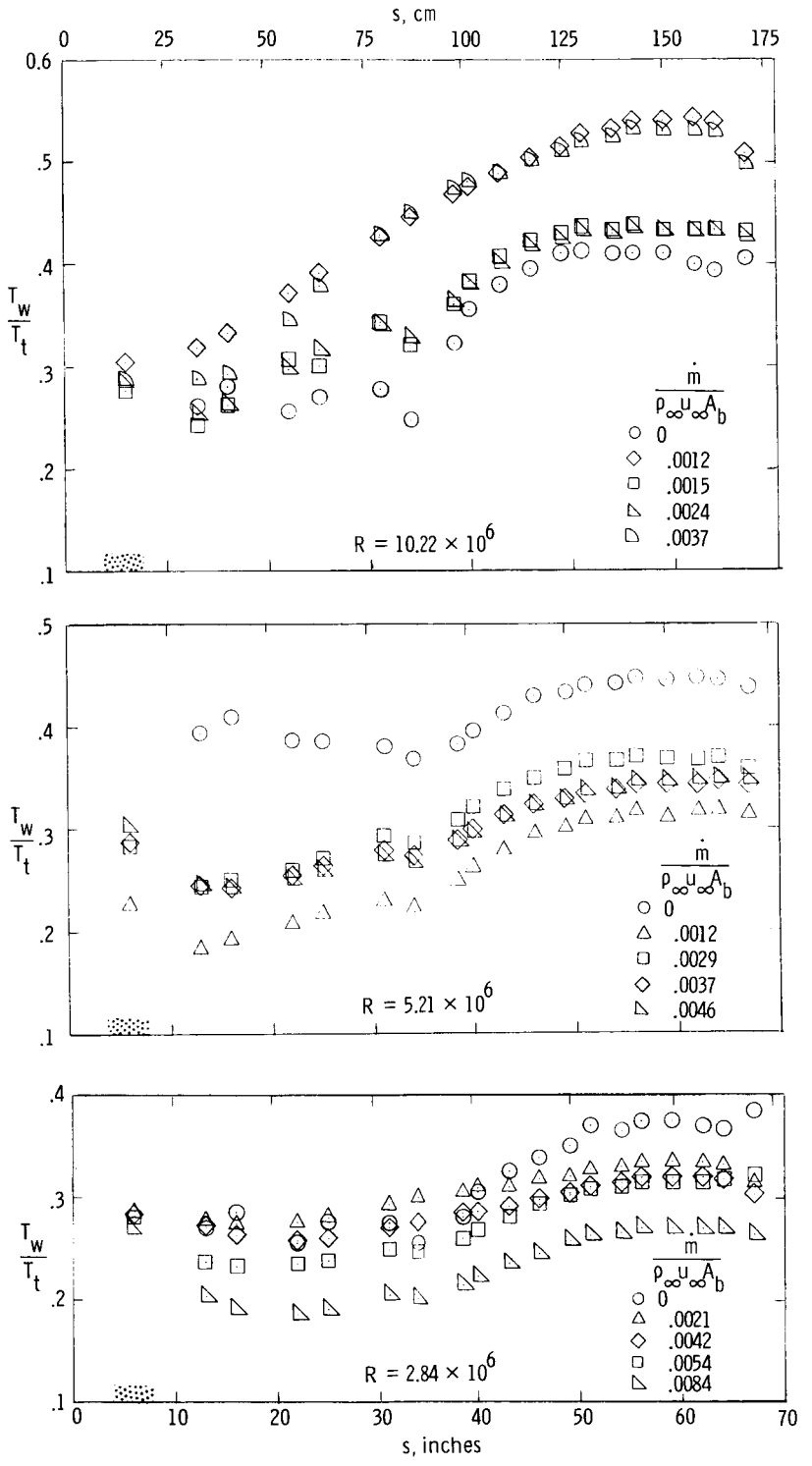

(b) Helium.

Figure 5.- Concluded.

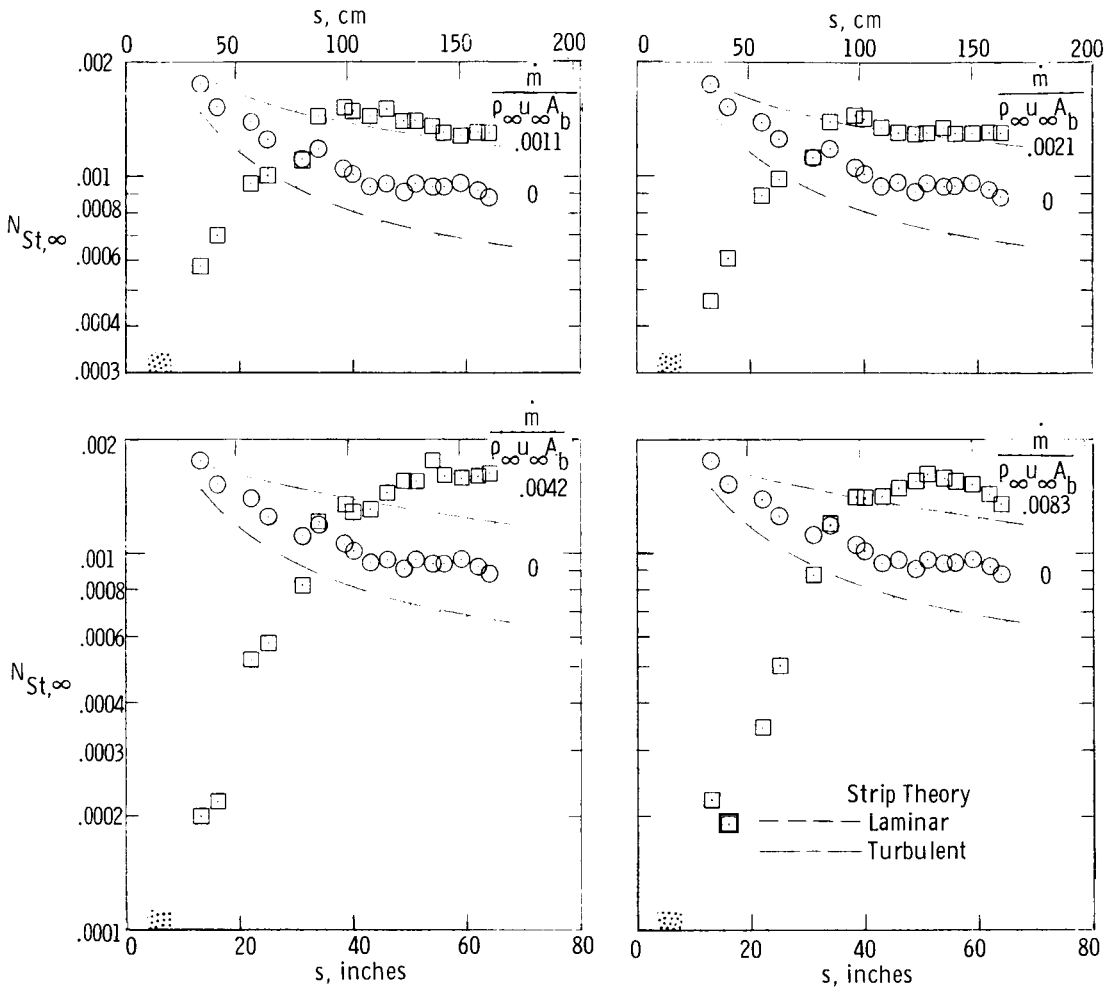

(a) $R = 2.84 \times 10^6$.

Figure 6.- Stanton number distribution for air transpiration.

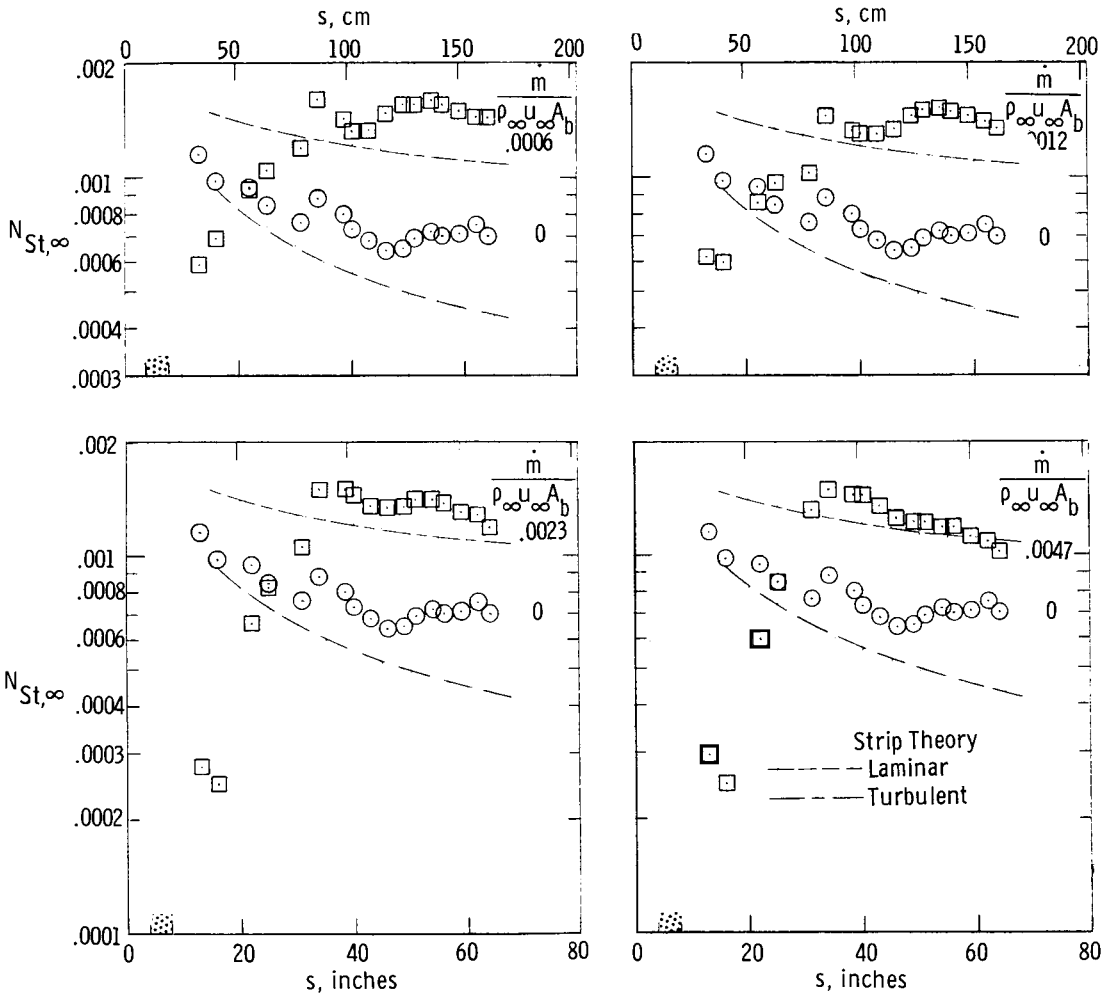

(b) $R = 5.21 \times 10^6$.

Figure 6.- Continued.

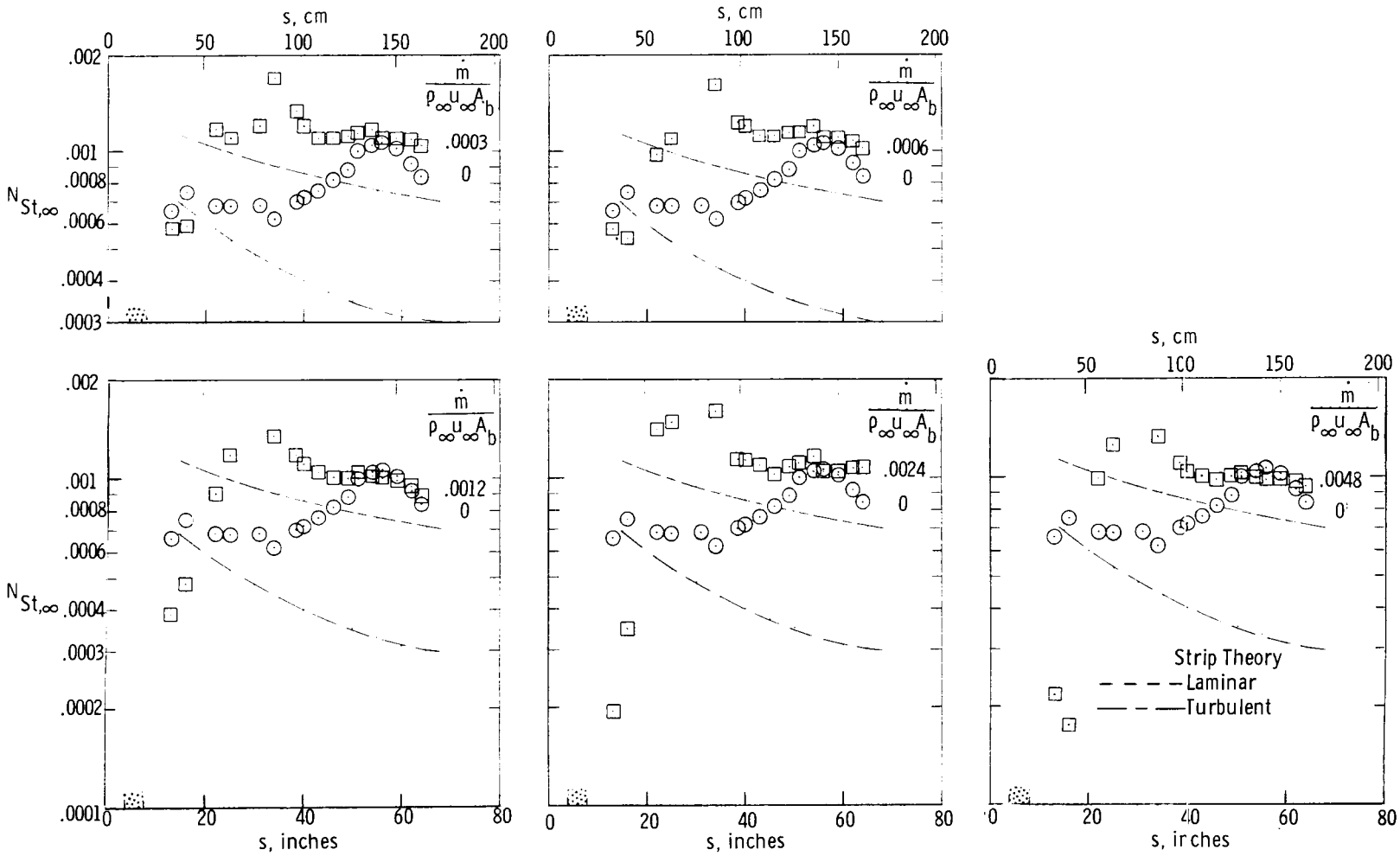

(c) $R = 10.22 \times 10^6$.

Figure 6.- Concluded.

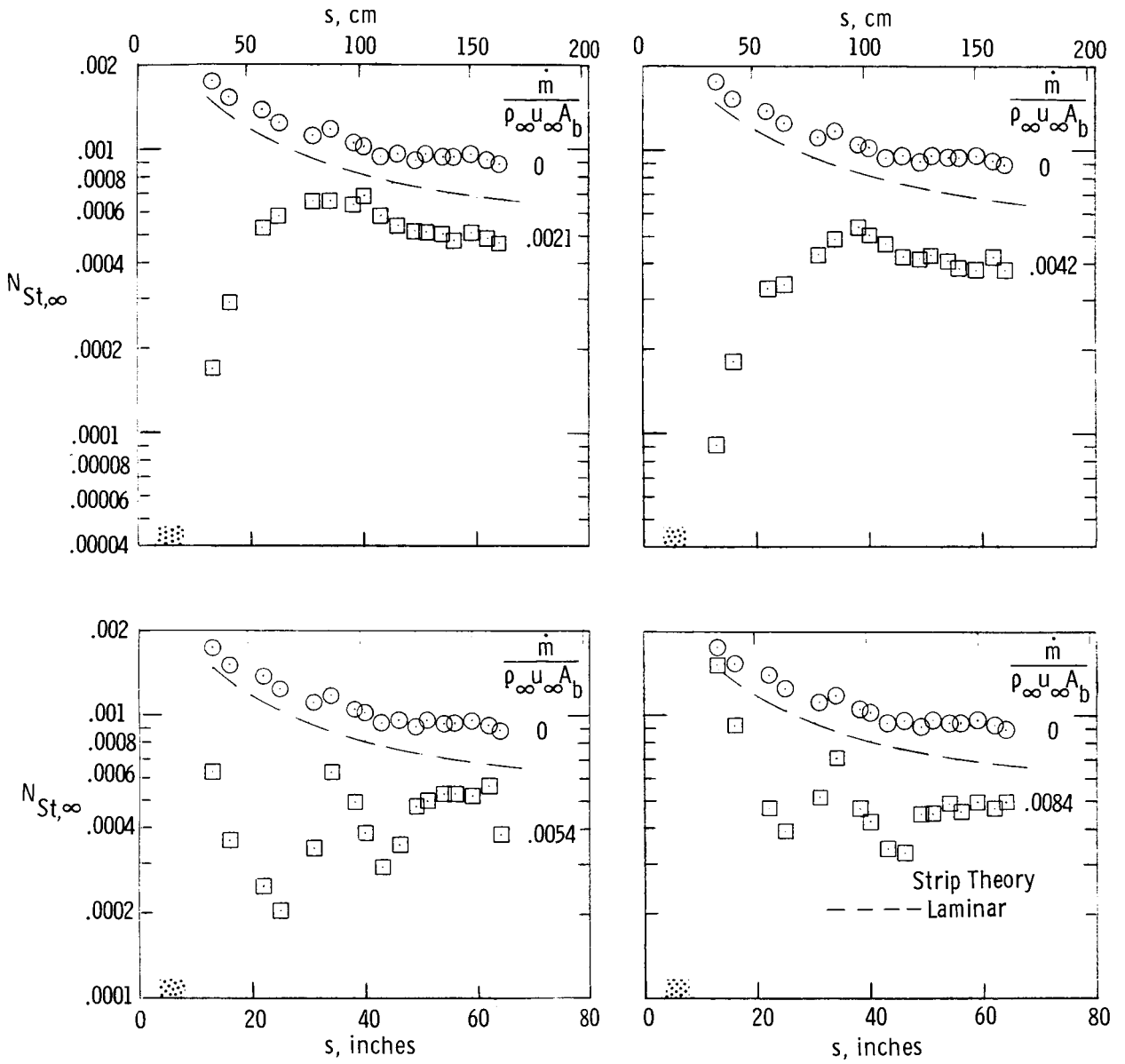

(a) $R = 2.84 \times 10^6$.

Figure 7.- Stanton number distribution for helium transpiration.

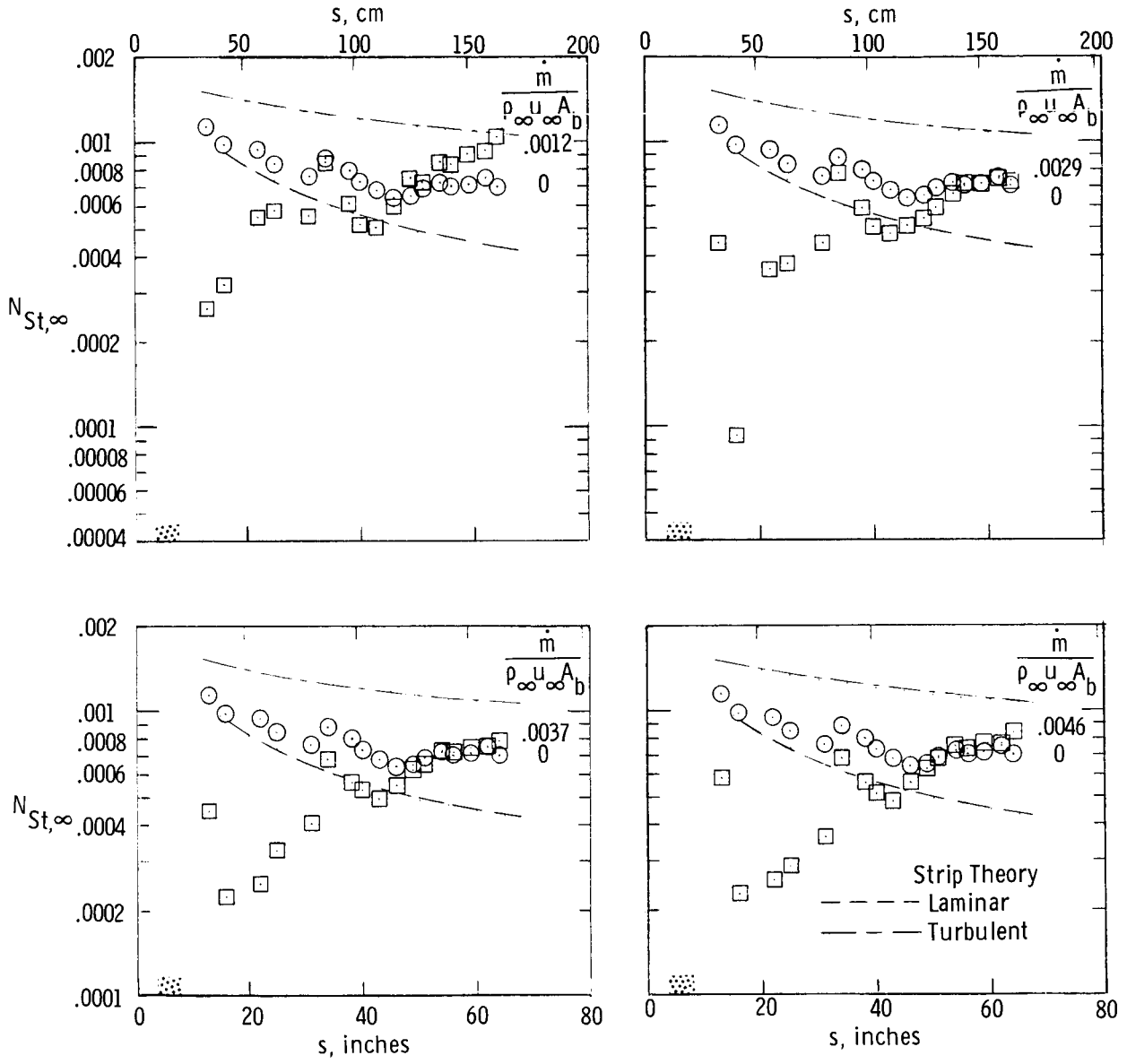

(b) $R = 5.21 \times 10^6$.

Figure 7.- Continued.

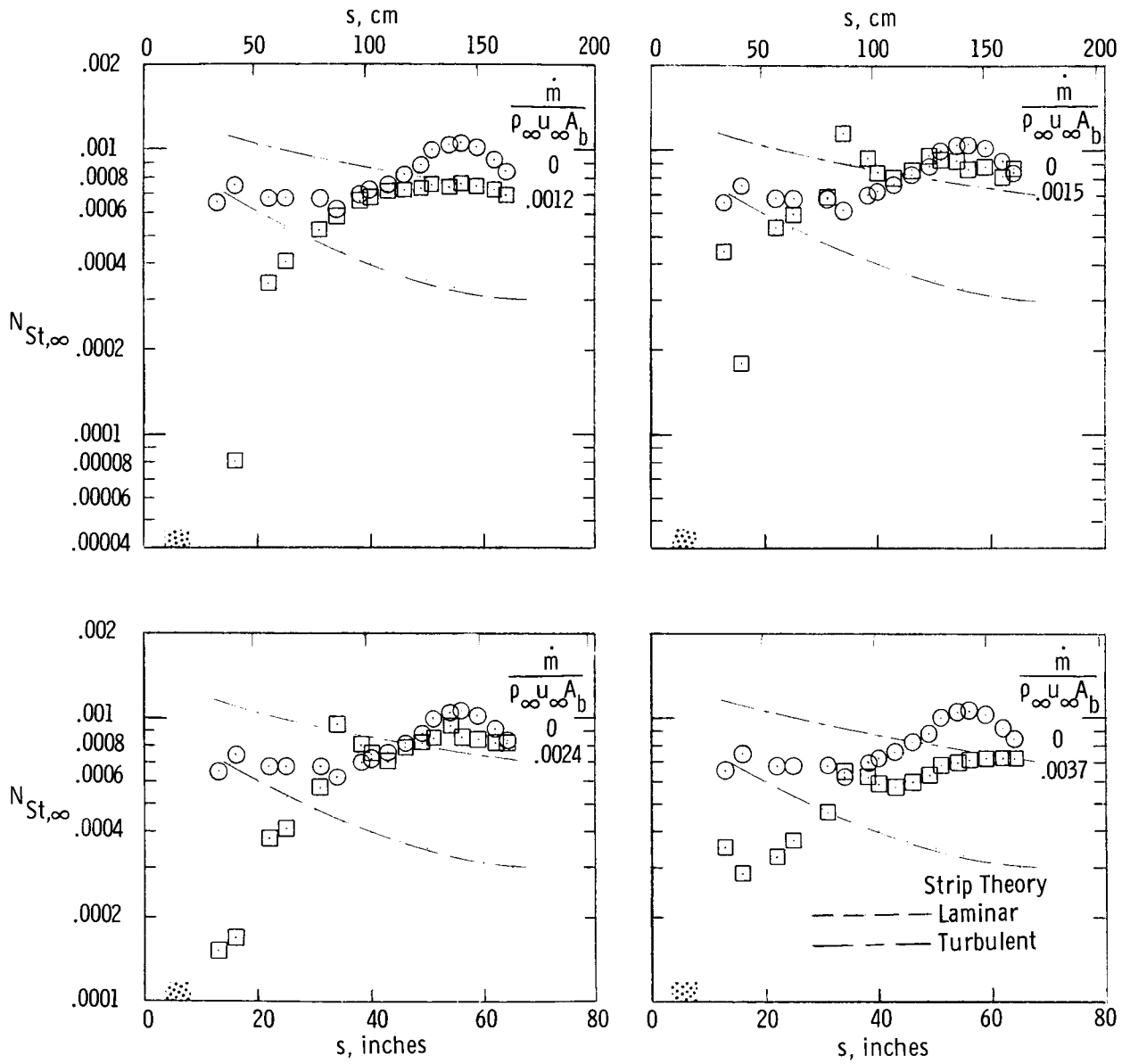

(c) $R = 10.22 \times 10^6$.

Figure 7.- Concluded.

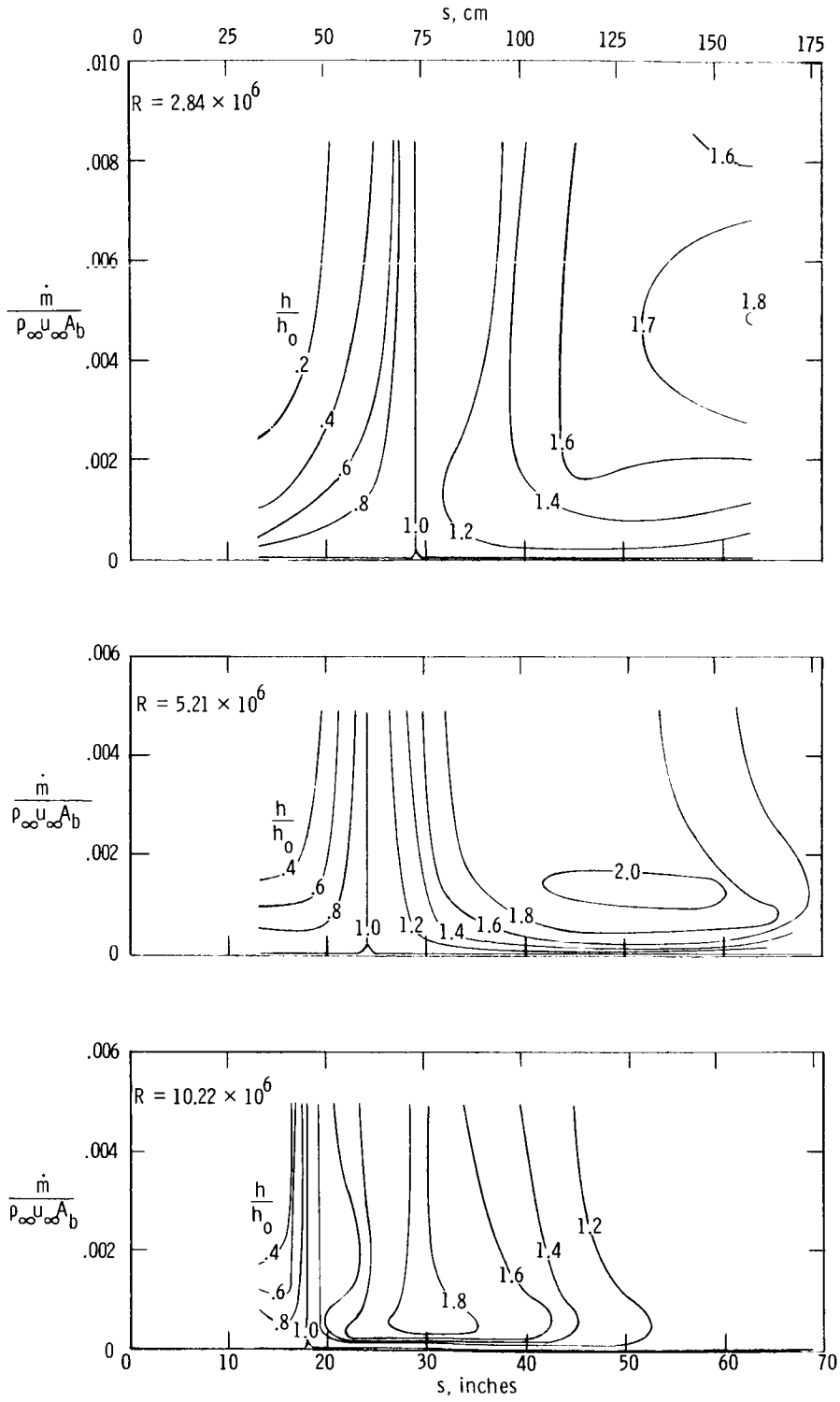

(a) Air.

Figure 8.- Contour plots of heat-transfer ratio h/h_0 on the cone surface.

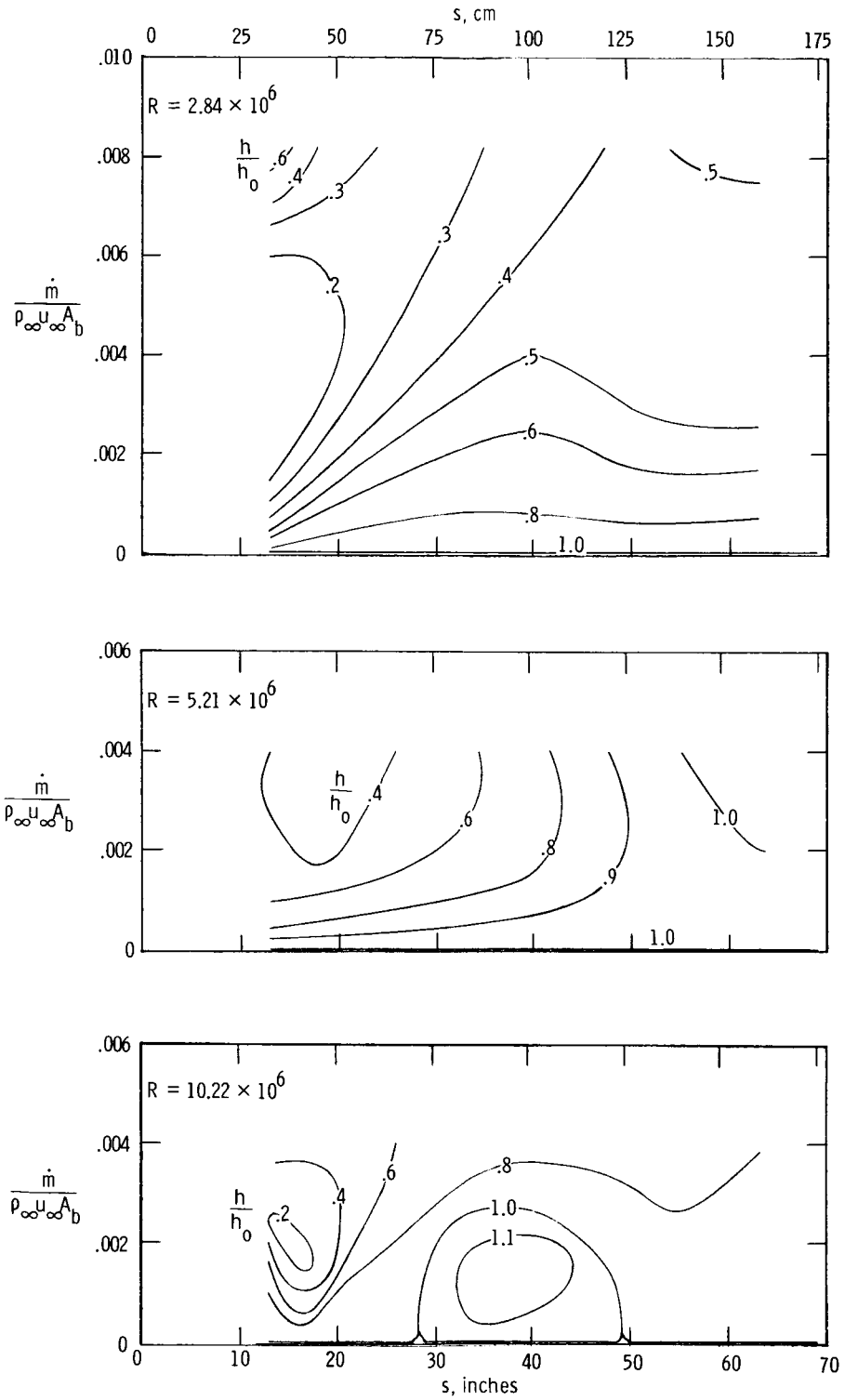

(b) Helium.

Figure 8.- Concluded.

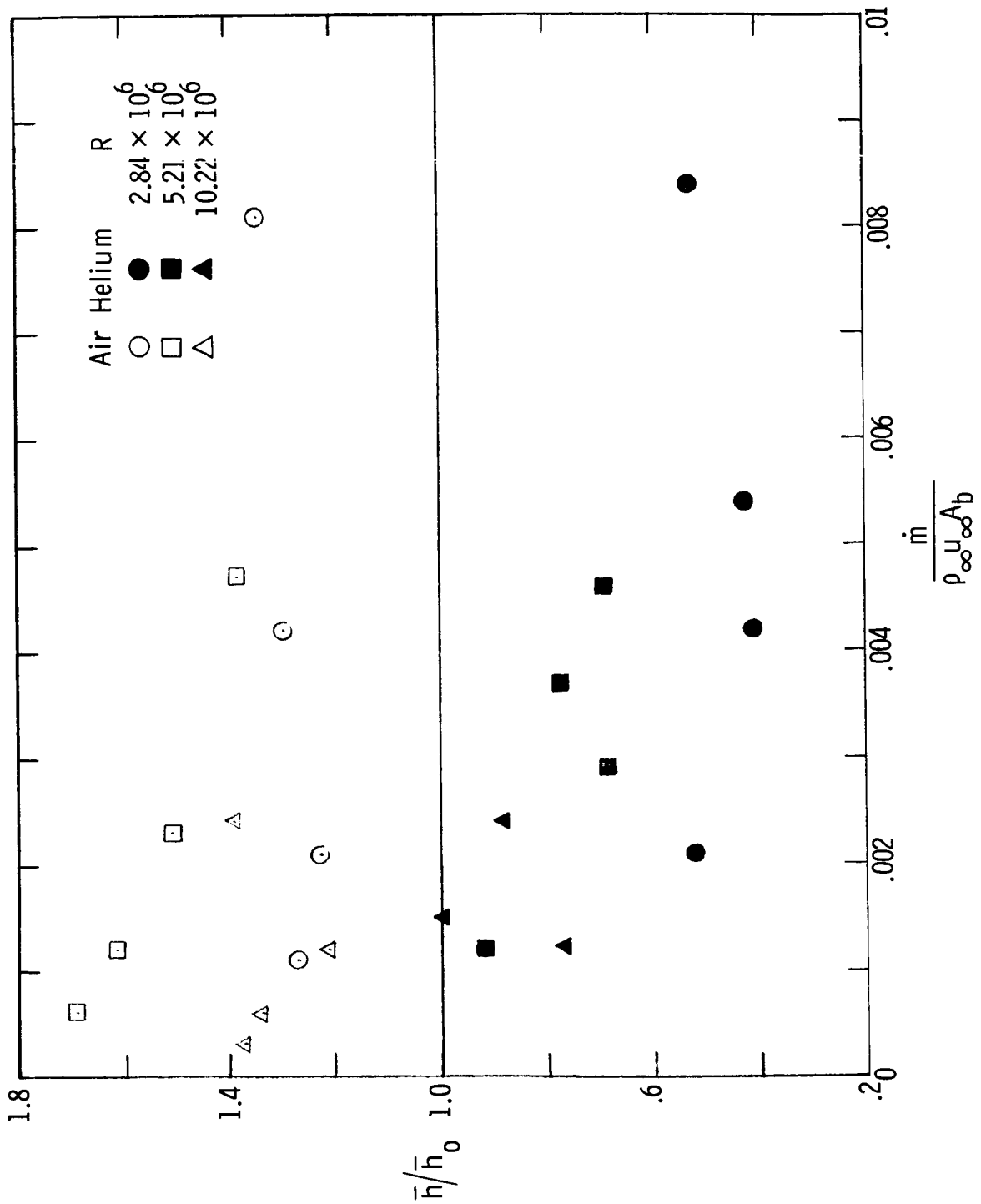

Figure 9.- Ratio of average heating to cone surface with transpiration to heating without transpiration.

NASA-Langley, 1969 —— 33 L-6161

1. Report No. NASA TN D-5554	2. Government Accession No.	3. Recipient's Catalog No.
4. Title and Subtitle EXPLORATORY HEAT-TRANSFER MEASUREMENTS AT MACH 10 ON A 7.5° TOTAL-ANGLE CONE DOWNSTREAM OF A REGION OF AIR AND HELIUM TRANSPIRATION COOLING		5. Report Date December 1969 6. Performing Organization Code
7. Author(s) James C. Dunavant and Philip E. Everhart		8. Performing Organization Report No. L-6161 10. Work Unit No. 124-07-12-04-23
9. Performing Organization Name and Address NASA Langley Research Center Hampton, Va. 23365		11. Contract or Grant No. 13. Type of Report and Period Covered Technical Note
12. Sponsoring Agency Name and Address National Aeronautics and Space Administration Washington, D.C. 20546		14. Sponsoring Agency Code

15. Supplementary Notes

16. Abstract

The heat transfer to a 7.5° total-angle cone at a Mach number of 10 was measured to determine the far downstream effects of injecting air and helium into the cone boundary layer through a porous section near the apex. Transpiration rates varied from 0.0003 to 0.0084 times the flow rate through a stream tube equal to the maximum diameter of the model. The transpiration of both air and helium at these rates produced large increases in the pressure ratio over the transpiration region and expansion just downstream of the porous section to pressures well below those measured without transpiration. Over the rear half of the cone, the surface pressures returned to within approximately 10 percent of the pressure on the cone without transpiration. Large decreases in the heating were obtained just downstream of the transpiration region and resulted from injection of even small masses of coolant. Boundary-layer transition occurred earlier with air transpiration but was unaffected by helium transpiration. Where the flow was already turbulent, transpiration of air did not decrease the heating rates but helium caused a small decrease.

17. Key Words Suggested by Author(s)	18. Distribution Statement
Transpiration cooling – air and helium Transition Heat transfer Aerodynamic heating Thermodynamic characteristics	Unclassified – Unlimited

19. Security Classif. (of this report)	20. Security Classif. (of this page)	21. No. of Pages	22. Price*
Unclassified	Unclassified	30	$3.00

*For sale by the Clearinghouse for Federal Scientific and Technical Information Springfield, Virginia 22151